

TWO-PHASE FLOW IN VERTICAL NONCIRCULAR CHANNELS

M. SADATOMI and Y. SATO

Department of Mechanical Engineering, Kumamoto University, Kumamoto, Japan 860

and

S. SARUWATARI

Department of Mechanical Engineering, Ariake Technical College, Omuta, Japan 836

(Received 25 January 1982; in revised form 23 April 1982)

Abstract—Experiments have been performed for vertical two-phase flow of air-water mixtures through several noncircular channels. Frictional pressure drops are discussed in terms of the correlation method for single-phase turbulent flow developed first in this study. Results for rising velocity of large gas bubble and mean void fraction are also discussed. Flow pattern boundaries are presented and compared with each other as to channel geometry.

INTRODUCTION

Noncircular channels through which two-phase gas-liquid mixtures flow are frequently used in engineering applications. In a cross section of a tube bundle or a rod bundle, for instance, several noncircular ones (subchannels) are present. However, most studies on two-phase flow to date are concerned with circular pipes and little is known about the flow characteristics in noncircular passages. It is desirable to obtain systematic knowledge of the flow mechanics in noncircular channels, not only for better understanding of the inherent flow behavior but also to make use of the information compiled from the investigation for round tubes so far made.

Data on two-phase pressure drop in noncircular channels are practically nonexistent. There is no guarantee that the correlation for circular pipes will continue to apply to noncircular ones. Therefore, an attention should be directed toward the pressure drop problem. In discussing two-phase frictional pressure drop in any noncircular channel, it is of importance to know a reasonable method for predicting that of single-phase flow in the channel considered. A literature survey concerning fully developed single-phase flows in straight noncircular passages reveals that knowledge of the laminar flow is satisfactory at least in engineering applications (Shah & London 1978), while that of the turbulent flow is still far from adequate to the need for various shapes encountered in practical systems. There is the well-known hydraulic diameter concept in this area; i.e. the pressure drop correlation which is valid for circular pipes may be applied to noncircular channels if the hydraulic diameter is substituted for the characteristic length in the friction factor and the Reynolds number (Nikuradse 1930). In recent years, however, there have been many experimental evidences that do not support this concept; for instance, Carlson & Irvine (1961), Gunn & Darling (1963). There is still a need to obtain the rational prediction method for the frictional pressure drop in other than circular pipes, particularly in the area of nuclear reactor engineering (Rehme 1973; Malák *et al.* 1975). Realizing these aspects, this investigation was then started with the consideration of frictional pressure drop for single-phase flow and followed by that for two-phase flow. The results of this investigation are reported in the present paper.

It is to be expected that the velocity of gas bubble in a two-phase flow will be influenced by flow behavior of the liquid phase that is probably accounted for by the channel shape. Measurements of the rising velocity of gas bubble were made in several noncircular channels:

rectangular, isosceles-triangular and concentric annular. The average void fraction was measured at the same time. The results are presented and discussed in this paper.

Information as to the flow pattern transition was also obtained in this investigation. Comparisons are made among such different shaped channels on the transitions of bubble-slug flow and slug-annular flow.

EXPERIMENT

Measurements of pressure drop, mean void fraction, cross-sectional distribution of void fraction, rising velocity of gas bubbles and flow pattern were performed for two-phase air-water flow in seven vertical channels. The pressure drop for single-phase water flows was also measured. Four channels were rectangular of different size, and the others were an isosceles-triangular, a concentric annular and a circular. Their dimension, cross-sectional area and hydraulic diameter are listed in table 1.

The circular pipe of 26 mm i.d. was served as a standard of comparison among the experimental data, for the fact that, in literature, there has been a great deal of information on two-phase flow obtained particularly in about one inch circular pipes. The cross-sectional area of both the isosceles-triangular and annular channels was chosen to be approximately equal to that of the circular one. The triangular one had an apex angle of 20 degree and a height of 55 mm, while the annular one consisted of a 30 mm i.d. tube and a rod of 15 mm dia. The three rectangular channels had short sides of 17, 10 and 7 mm respectively with equal long sides of 50 mm. The cross section of the remainder was 7×20.6 mm having the same aspect ratio to the 17×50 mm one (1:2.94). As a whole, the hydraulic diameter of the seven channels ranged from 10.4 to 26 mm; that of the circular and the 17×50 mm rectangular ones and that of the triangular and the 10×50 mm rectangular ones were quite similar to each other, respectively.

A sketch of the essential part of the test rig is shown in figure 1. The test sections were made of acrylic resin plates or tubes with a smooth wall surface. After leaving a calibrated orifice, water flowed into a test section at the bottom end, then reached a two-phase mixer. Following a rotameter, air was injected into a water stream through the mixer, in which there were a number of holes (distributed by 11-holes/cm² of the cross section) drilled on the periphery of the channel wall. The diameter of these air holes was either 0.3 or 2.0 mm depending on the magnitude of air flow rate. Then, two-phase mixture flowed upward in an entrance section of length L_2 and passed through a measuring section of L_1 , in which the pressure drop, the mean void fraction, the cross-sectional distribution of void fraction and the rising velocity of gas bubbles were measured. After leaving the measuring section, the mixture passed through an exhaust section of L_3 , and finally discharged into a separator. Separated air then issued into the atmosphere, while the drainage was led to a weighing tank to check the flow rate. Exit water temperature was read from a mercury-in-glass thermometer placed in the tank. This temperature was used to evaluate physical properties of air as well as water. The values of L_1 , L_2 and L_3 of each channel are shown in table 1.

Table 1. Dimensions of test sections

| shape | dimension mm | area | | hydraulic dia. | | length | | |
|-------|-----------------|-------------------|------------------|-------------------|--------------------------------|------------------|------------------|------------------|
| | | A mm ² | A/A _o | D _h mm | D _h /D _o | L ₁ m | L ₂ m | L ₃ m |
| □ | 17×50 | 850 | 1.60 | 25.4 | 0.98 | 1.1 | 2.4 | 1.2 |
| | 10×50 | 500 | 0.94 | 16.7 | 0.64 | 1.1 | 1.8 | 1.2 |
| | 7×50 | 350 | 0.66 | 12.3 | 0.47 | 1.1 | 1.5 | 0.9 |
| | 7×20.6 | 144 | 0.27 | 10.4 | 0.40 | 1.1 | 1.5 | 0.9 |
| △ | 20°, h=55 | 533 | 1.01 | 16.3 | 0.63 | 1.1 | 2.4 | 1.2 |
| ⊙ | φ15/φ30 | 530 | 1.00 | 15.0 | 0.58 | 1.3 | 1.5 | 0.8 |
| ○ | φ26 | 531 | 1 | 26.0 | 1 | 1.7 | 3.2 | 1.2 |

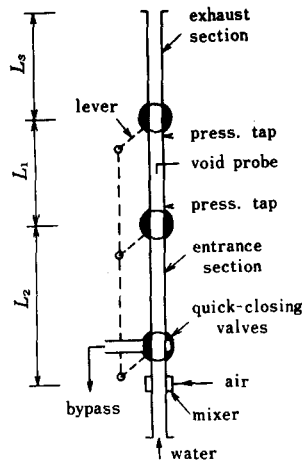


Figure 1. Schematic sketch of an experimental apparatus.

Mean void fraction was obtained by the well-known quick-closing valve technique; the volume of water, trapped by the two isolation cocks arranged at both ends of the measuring section, was measured. Special care was taken in the fabrication of a cylindrical rotation plug in such a cock; i.e. the flow passage was grooved perpendicularly to the plug and finished so as to be flush with the passage of channel just before and behind it. For the annular channel, a piece of 15 mm dia. core rod was concentrically held by pins in the 30 mm dia. circular passage. To obtain accurate void fraction data, especially in a case of a slug flow, twenty or more operations were performed.

Pressure gradient was obtained from the static pressure difference Δp between two taps placed in the measuring section at an interval of $\Delta x = 0.75 \sim 1.0$ m. This pressure differential was measured by means of an inverted water/air manometer and a traveling microscope. A capillary vinyl tube of 1.4 mm i.d. of reasonable length was laid within the pressure leads, eliminating undesirable fluctuations of meniscus in the manometer. Frictional pressure gradient in two-phase flow was determined from the static pressure gradient $\Delta p/\Delta x$ by means of the following equation, assuming that the accelerational pressure gradient and the weight of air are negligible:

$$\frac{\Delta p_f}{\Delta x} = \frac{\Delta p}{\Delta x} - \rho_L g (1 - \alpha) \quad [1]$$

where ρ_L , g and α are the liquid density, the gravitational acceleration and the mean void fraction respectively.

In the annular channel, the core rod was concentrically held by the three 2 mm o.d. radial pin spacers, arranged every 0.5 m interval along the axis. Then, there were two sets of the spacers between the taps, which might be considered as flow obstructions. However, their effect on the pressure drop seemed to be small from the experimental facts that in single-phase water flow there was no remarkable difference between the pressure gradients with and without the spacers.

Rising velocity of large gas bubbles, a solitary gas bubble as well as successive gas bubbles in two-phase slug flow, was measured by a double needle-contact probe of the type commonly used in two-phase flow experiments. One of these probes was also used for the measurements of cross-sectional distribution of void fraction and for the flow pattern detection. The method for the determination of flow pattern will be described in the later chapter.

RESULT AND DISCUSSION

Pressure drop

This section begins with the treatment of single-phase pressure drop in noncircular channels; the relation between friction factor and channel geometry is described for both laminar and turbulent flows. There then follows the description of two-phase pressure drop; two-phase flow data are correlated in terms of the two-phase frictional multiplier.

(a) *Single-phase flow.* If hydraulic equivalent diameter D_h and corresponding friction factor λ are introduced, the relation between frictional pressure gradient $\Delta p_f/\Delta x$ and mean velocity \bar{u} is written as the conventional Darcy's formula;

$$\frac{\Delta p_f}{\Delta x} = \lambda \frac{1}{D_h} \frac{\rho \bar{u}^2}{2}. \quad [2]$$

However, as already mentioned in the introduction, it is found experimentally that the friction factor vs Reynolds number relationship as it has been proposed for circular channel is not necessarily valid for noncircular one, even if D_h alone is substituted for the diameter; Carlson & Irvine (1961), Gunn & Darling (1963), Aly *et al.* (1978). This suggests that the friction factor defined by [2] depends also on the channel geometry considered. It may be profitable to obtain a correlation between friction factor and channel geometry.

As for fully developed laminar flow in a straight channel of constant cross-sectional area, the pressure gradient can be calculated by a numerical method. The Navier–Stokes equation for fully developed laminar flow in the x -direction under steady state conditions becomes:

$$\frac{\partial^2 u}{\partial y^2} + \frac{\partial^2 u}{\partial z^2} - \frac{1}{\mu} \frac{\partial p_f}{\partial x} = 0 \quad [3]$$

where u is velocity in the x -direction, and μ is dynamic viscosity. If the partial differential equation [3] is approximated by a finite difference expression, the flow can be solved numerically (e.g. by successive over-relaxation method) for a given pressure gradient under the boundary condition of the no-slip at the wall; i.e. the velocity profile is determined. Then, the relation between the pressure gradient and the mean velocity is obtained. As expected, substitution of these values into [2] results in [4] as the friction factor vs Reynolds number relationship in the channel,

$$\lambda = C_l \text{Re}^{-1} \quad [4]$$

where

$$\text{Re} = \rho \bar{u} D_h / \mu. \quad [5]$$

The proportionality constant C_l is called geometry factor for laminar flow, because it is determined solely by the boundary condition and the geometry of channel cross section (e.g. Rehme 1971). C_l for various channels has already been reported by several investigators, and, in particular, the book of Shah & London (1978) contains C_l -tables for various kinds of channel geometry.

Figure 2 shows the calculated results of the relative geometry factor C_l/C_{l0} for isosceles-triangular, rectangular and concentric annular channels; relative to that of circular channel ($C_{l0} = 64$). Each curve is drawn against characteristic value for geometry. The C_l/C_{l0} value for isosceles-triangular is less than unity and *vice versa* for concentric annular. The maximum value of C_l/C_{l0} occurs in parallel flat plates.

For turbulent flow, in general, the friction factor is unable to be determined by purely theoretical calculation. Then, experimental data of the friction factor for fully developed

turbulent flow in noncircular channels are examined here, and an attempt is made to correlate it with the channel geometry. Both figures 3(a) and (b) show the friction factors obtained experimentally for concentric annular, rectangular, isosceles-triangular channels with a smooth wall plotted against Reynolds numbers defined by [5]; figure (a) is concerned with the present experiment, while figure (b) the experiments of other investigators; Quarmby (1967), Hartnett *et al.* (1962) and Carlson & Irvine (1961). Logarithm scale co-ordinates are employed as usual. The experimental data are labeled according to the channel shape. Several lines corresponding to each channel are also drawn, the theoretical calculations in laminar flow region and the best-fit lines to data points in turbulent flow region. In addition, $\lambda = 64/Re$ and the Blasius formula are plotted respectively for both flow regions by a solid line.

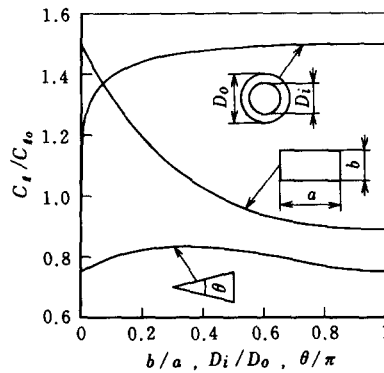
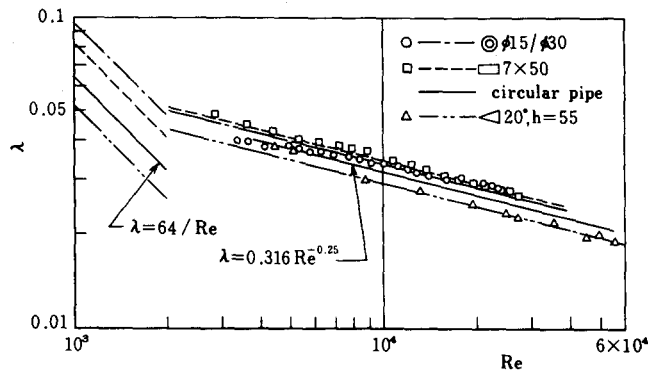
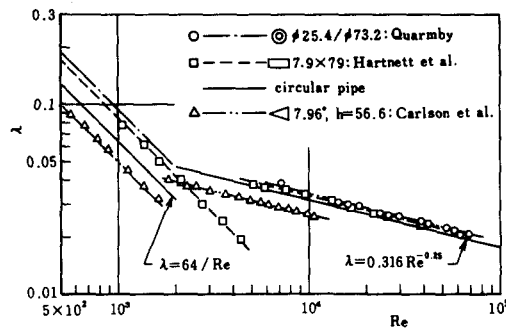


Figure 2. Relative laminar geometry factor C_l/C_{l0} for various channel geometries.



(a)



(b)

Figure 3. Friction factor and Reynolds number relationship for several noncircular smooth test sections: (a) present experiment; (b) data of other investigators.

It is evident from these figures that in the laminar flow region the agreement between the theoretical calculations and data points of Hartnett *et al.* and Carlson & Irvine is excellent, and in the turbulent flow region the data points are found to follow the best-fit lines whose slope is equal to -0.25 being parallel to the Blasius formula. As for the available data of noncircular channels with a smooth wall other than those quoted in figure 3, the similar trend is seen to hold for friction factors in turbulent flow region as held in the figures; Gunn & Darling (1963), Tiedt (1968), Lawn & Elliott (1972), Jones, Jr. (1976) and Aly *et al.* (1978). (Only in a case of annular passage it appears that data tend to fall a line having the slope of -0.2 rather than -0.25 ; for instance, the present experiment shown in figure 3(a) and Jonsson & Sparrow (1966). However, the slope of -0.25 seems to be suitable also for them within a tolerable difference.) Consequently, friction factor for any channel with a smooth wall can be correlated by the following power-law equation similar to Blasius:

$$\lambda = C_t \text{Re}^{-0.25}. \tag{6}$$

The coefficient C_t alone represents channel geometry since the exponent of Reynolds number can be fixed to be -0.25 . Then, for convenience sake C_t will be termed as "geometry factor for turbulent flow", analogous to C_l in [4].

Such turbulent geometry factors for several noncircular channels has been determined from reliable experimental data referred to in the previous paragraph, giving priority to those being in the Reynolds number range between 10^4 and 10^5 , and examined for its dependence on the geometry factor for laminar flow. The results are presented in figure 4 with C_t/C_{t0} as ordinate and C_l/C_{l0} as abscissa, in which suffix 0 denotes circular pipe. Three data points plotted at the extreme left in the figure correspond to the test channels of Gunn & Darling whose cross sections are analogous to ones seen in closely-packed square-array rod bundles. The other data points are labeled according to both the investigator and the channel geometry; squares to rectangular, triangles to isosceles-triangular and circles to annular channels. The extent of C_l -value for each geometry is indicated by a segment parallel to the abscissa. Figure 4 indicates that there is such a close relationship between C_t and C_l as shown by the solid curve, which can be approximated by

$$\frac{C_t}{C_{t0}} = \sqrt[3]{\left(0.0154 \frac{C_l}{C_{l0}} - 0.012\right) + 0.85}. \tag{7}$$

Hence, for a given channel geometry C_t can be estimated by [7] once C_l has been obtained

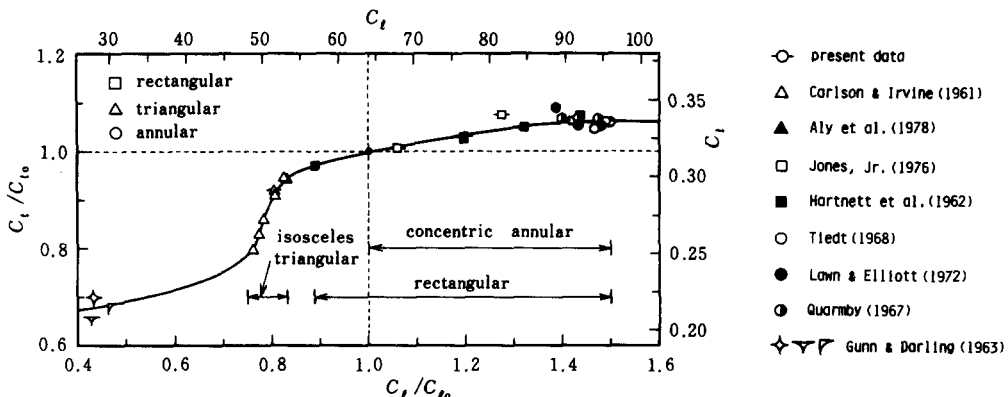


Figure 4. Relation between turbulent geometry factor C_t and laminar geometry factor C_l .

from either available data in literature or a numerical calculation. Then, the friction factor for turbulent flow can be determined.

(b) *Two-phase flow.* An attempt was made to correlate the present data by means of the Lockhart & Martinelli parameters (Lockhart & Martinelli 1949) defined by

$$\phi_L = \sqrt{\left(\frac{(\Delta p_f/\Delta x)}{(\Delta p_f/\Delta x)_L}\right)} \quad [8]$$

$$\chi = \sqrt{\left(\frac{(\Delta p_f/\Delta x)_L}{(\Delta p_f/\Delta x)_G}\right)} \quad [9]$$

where $(\Delta p_f/\Delta x)$ is the frictional pressure gradient for two-phase flow, and $(\Delta p_f/\Delta x)_G$ and $(\Delta p_f/\Delta x)_L$ are those for the gas and liquid phases respectively flowing alone within the same channel. For a noncircular channel, both $(\Delta p_f/\Delta x)_G$ and $(\Delta p_f/\Delta x)_L$ can be calculated by the method proposed in the above section. Figures 5(a)–(c) show the results for the three channels except the rectangular channels whose data were quite similar to those demonstrated in figures 5(a) and (b). Data points are labeled according to superficial liquid velocity j_L and also to combination of the modes of the superficial liquid and gas flow; e.g. a point \ominus (ϕ_{Ltt}) is the case where a flow of the liquid phase alone is turbulent and that of the gas phase alone is laminar. Both geometry factors, C_1 and C_b , are shown in each figure. In addition, the Lockhart & Martinelli ϕ_{Ltt} -curve and the Chisholm & Laird correlation (Chisholm & Laird 1958),

$$\phi_{Ltt}^2 = 1 + \frac{21}{\chi} + \frac{1}{\chi^2} \quad [10]$$

are represented by the dashed and the solid curve respectively in the figures.

The data in figure 5(c) only exhibit considerable scatter, which may be due to possible errors caused by the measurement of void fraction. However, study of these figures reveals in general that it is promising to rely on the Lockhart & Martinelli parameters for correlating the experimental results for noncircular channels as well as circular pipes if an appropriate value for both $(\Delta p_f/\Delta x)_G$ and $(\Delta p_f/\Delta x)_L$ can be obtained, and, furthermore, that it may be preferable to use the Chisholm & Laird correlation, [10], for predicting such frictional pressure gradient with sufficient accuracy for most practical purposes.

Rising velocity of large gas bubbles

(a) *A solitary air bubble in moving water streams.* In this experiment solitary air bubbles ranging (5 ~ 15) D_h in length were injected into water streams and the rising velocity was measured. Each measured velocity was corrected for elongation of the bubble due to change of static pressure as it rose. As a result, it was found that the length of an air bubble had little effect on the velocity.

Figure 6 shows the typical results for the triangular and the 7 × 50 mm rectangular channels. It is evident from the figure that the rising velocity u_G increases linearly with mean water velocity \hat{u} , and the slope varies with channel geometry; i.e. the slope for the isosceles-triangular channel is steeper than that for the rectangular one. The rising velocity of an air bubble in a noncircular channel may therefore be correlated by

$$u_G = C_1 \hat{u} + u_{GO}, \quad [11]$$

in which u_{GO} is the velocity in the stagnant water column.

It is known that in circular pipes the value of C_1 is about 1.2 and is close to the ratio of the maximum to mean velocity u_m/\hat{u} for fully developed turbulent flow; e.g. Nicklin *et al.* (1962).

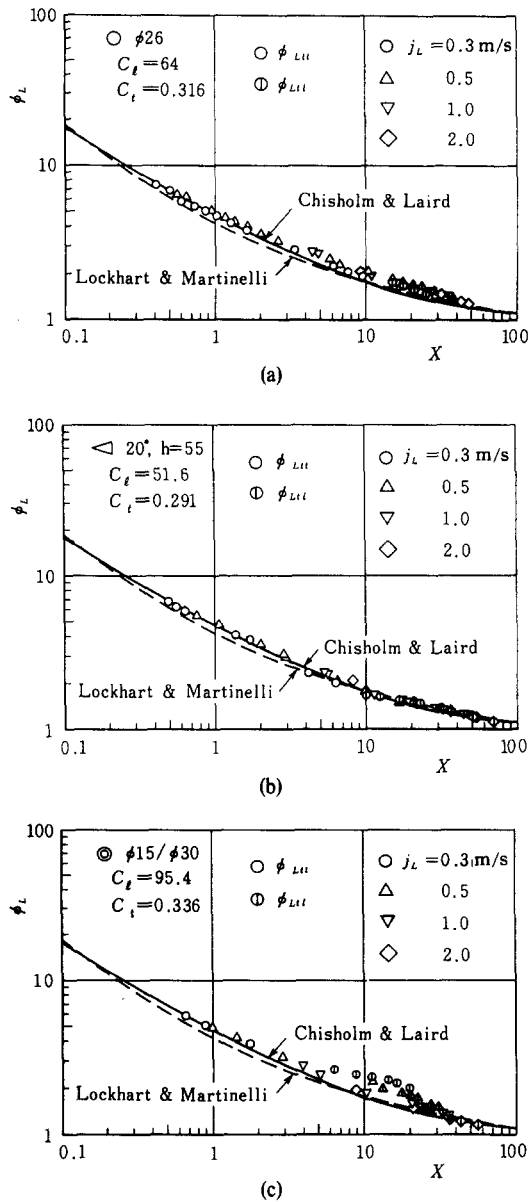


Figure 5. Two-phase frictional pressure gradient.

Then, as for the significance of C_1 there has been an anticipation that C_1 may be equal to u_m/\hat{u} even for noncircular channels. From this interpretation, Griffith (1964) calculated u_m/\hat{u} -value for rectangular channel and annuli assuming the power-law velocity profile. However, he was unable to compare his calculation directly to the velocity of gas bubble. Thus, conclusive interpretation of the coefficient C_1 has not yet been obtained.

In order to examine experimentally such interpretation that $C_1 \approx u_m/\hat{u}$, the maximum velocity u_m was measured by means of a pitot tube. The results for the six channels are shown in figure 7 as a function of Reynolds number. For a Reynolds number greater than 2×10^4 , the ratio u_m/\hat{u} is virtually independent of Re . Comparisons of u_m/\hat{u} at $Re = 2 \times 10^4$ with C_1 are shown in table 2. The agreement between the two can be considered satisfactory though additional experimental information is needed for annular channel.

(b) *A solitary air bubble in a stagnant water column.* An experiment for determination of u_{GO} in [11] was run in several channels filled with stagnant water. The results are shown in

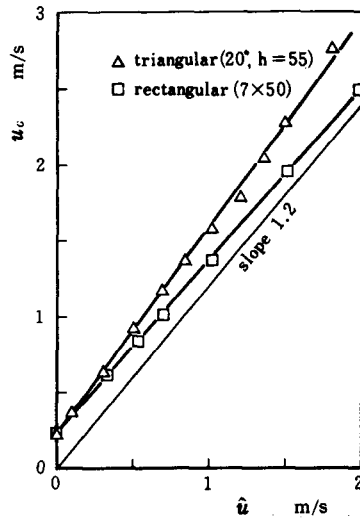


Figure 6. Rising velocity of a solitary gas bubble in moving water streams. ($\Delta 20^\circ$, $h = 55$ and $\square 7 \times 50$.)

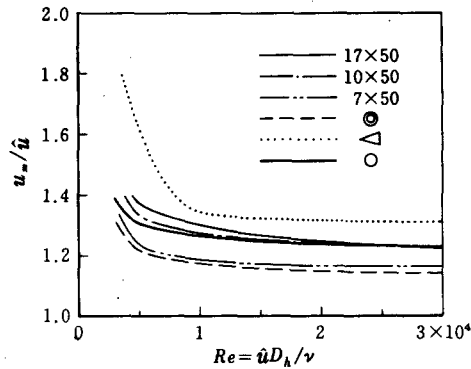


Figure 7. Ratio of maximum to mean velocity vs Reynolds number.

table 3. Also shown in the table are the measurements of Griffith (1964) and the additional data of the authors for rectangular channels of 30×30 mm and 30×120 mm. Since only gravity and inertia forces are the dominant parameter in a relatively larger channel filled with water, it is expected that u_{GO} can be correlated by the following Froude-number-type expression,

$$C_2 = \frac{u_{GO}}{\sqrt{(gD)}} \quad [12]$$

where D is the characteristic dimension.

It is known that for a circular pipe $C_2 = 0.35$, Dumitrescu (1943) and Davis & Taylor (1950). For a noncircular channel, however, a question has arisen as to the characteristic dimension D . Griffith (1964) reports that the large dimension is most important in channels; for instance, the shroud dimension in annuli and tube bundles. However, it is felt that the large dimension is not decisive because the resulting C_2 is still dependent on channel geometry. Then, in the present study an equi-periphery diameter D_e , which is equivalent to the quotient of the periphery divided by π , was tested as the characteristic dimension. The results, $C_2 = u_{GO}/\sqrt{(gD_e)}$, are presented in table 3. Almost all data are in the range from 0.31 to 0.36 except for the two cases. When a Eötvös number, $\rho_L g D_e^2 / \sigma$, is greater than 70, as is the cases of the present experiment,

Table 2. Comparison between C_1 and u_m/\hat{u} at $Re = 2 \times 10^4$

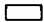








| shape | dimension mm | C_1 | u_m/\hat{u} |
|---|-----------------|-------|---------------|
|  | 17×50 | 1.20 | 1.23 |
| | 10×50 | 1.24 | 1.23 |
| | 7×50 | 1.16 | 1.17 |
| | 7×20.6 | 1.21 | 1.23 |
|  | 20°, h=55 | 1.34 | 1.31 |
|  | φ15/φ30 | 1.30 | 1.15 |
|  | φ26 | 1.25 | 1.23 |

Table 3. Rising velocity of a solitary gas bubble in a stagnant water column

| shape | dimension mm | $D_e^{*})$ mm | u_{GO} m/s | $u_{GO}/\sqrt{gD_e}$ | shape | dimension mm | $D_e^{*})$ mm | u_{GO} m/s | $u_{GO}/\sqrt{gD_e}$ |
|---|---------------------------|------------------|-----------------|----------------------|---|---|------------------|-----------------|----------------------|
|  | 7×20.6 | 17.6 | 0.142 | 0.34 |  | 20°, h=55 | 41.7 | 0.214 | 0.33 |
| | 8.9×37.8 ^{+))} | 29.7 | 0.167 | 0.31 | |  | φ15/φ30 | 45.0 | 0.211 |
| | 7×50 | 36.3 | 0.228 | 0.38 | φ5.9/φ50.8 ^{+))} | | 56.7 | 0.247 | 0.33 |
| | 10×50 | 38.2 | 0.204 | 0.33 | φ12.3/φ50.8 ^{+))} | | 63.1 | 0.272 | 0.35 |
| | 30×30 | 38.2 | 0.207 | 0.34 | φ17.8/φ50.8 ^{+))} | | 68.6 | 0.272 | 0.33 |
| | 17×50 | 42.7 | 0.216 | 0.33 |  | φ3.9×7/φ50.8 ^{+))} | 77.8 | 0.267 | 0.31 |
| | 37.6×50.3 ^{+))} | 56.0 | 0.232 | 0.31 | | φ6.6×7/φ50.8 ^{+))} | 97.0 | 0.310 | 0.32 |
| | 51.6×52.1 ^{+))} | 66.0 | 0.254 | 0.32 | | φ10×7/φ50.8 ^{+))} | 121 | 0.429 | 0.39 |
| | 11.0×133 ^{+))} | 91.9 | 0.292 | 0.31 |  | φ26 | 26.0 | 0.181 | 0.36 |
| | 30×120 | 95.5 | 0.336 | 0.35 | | φ50.8 ^{+))} | 50.8 | 0.240 | 0.34 |

*) equi-periphery diameter; D_e = periphery/ π

+) from the measurements performed by Griffith (1964)

White & Beardmore (1962) showed that the effect of both surface tension and viscous forces are negligible. Accordingly, it can be concluded that, when the Eötvös number exceeds 70, [12] is applicable to noncircular channels if the equi-periphery diameter D_e is substituted for D .

(c) *Successive air bubbles in two-phase slug flow.* The results for solitary air bubble mentioned in the preceding paragraphs suggest that the rising velocity of two-phase gas bubbles in noncircular channels can also be described by the currently used equation of Griffith & Wallis (1961) and Nicklin *et al.* (1962) for circular channel:

$$u_G = C_1(j_G + j_L) + u_{GO} \quad [13]$$

where j_G and j_L are the superficial velocities of gas and liquid respectively. Comparisons of the rising velocities predicted by [13] with those obtained experimentally are shown in Figs. 8(a) and (b), for the isosceles-triangular and the 17×50 mm rectangular channels. From such comparison, it can be said that the rising velocity of two-phase gas bubble in noncircular channels is closely approximated by [13] along with $C_1 = u_m/\hat{u}$ and $u_{GO} = 0.35 \sqrt{gD_e}$.

However, it should be emphasized that there may be a limit for these equations to be used for tube bundles or channels consisting of asymmetry, parallel subchannels. Griffith (1964) reports that in tube bundles with relatively larger tubes a marked channeling occurs, which is characterized by partition of the passages between tubes into two sorts, ones consisting almost entirely of gas and the rest consisting almost entirely of liquid. It may be expected for these phenomena to persist particularly in a flow with moderate mean void fraction and phase velocities, to occur more easily with an increase of the number of rods and their diameter and to cause an increase in bubble rise velocity. Under conditions where such a channeling prevails,

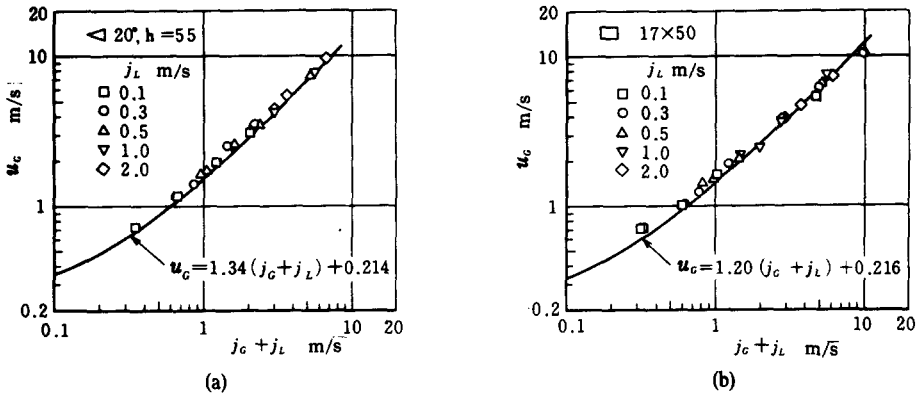


Figure 8. Comparison of [13] with experimental data of the velocity of gas bubble in two-phase slug flow.

the coefficient C_1 in [11] and [13] will not be consistent with u_m/\hat{u} and, in addition, $C_2 = u_{G0}/\sqrt{(gD_e)}$ will not remain constant to be about 0.35. Regarding the latter C_2 , inspection of the data of Griffith on the tube bundles presented in table 3 suggests that $u_{G0}/\sqrt{(gD_e)}$ slightly increases with increasing rod diameter at a fixed shroud diameter even though D_e is employed.

Void fraction

(a) *Mean void fraction.* Relation of the mean void fraction, the superficial velocity and the gas velocity in a two-phase flow is expressed by

$$\alpha = \frac{j_G}{u_G} \tag{14}$$

If [13] is used for u_G , the void fraction in slug flow can be calculated. In this study comparisons were made between α and the measurements α_{exp} obtained by a quick-closing valve method. The two typical results are presented in figures 9(a) and (b). It can be seen from the figures that, in the range of $\alpha_{exp} < 0.8$ including not only slug flow but also bubble flow regime of $\alpha_{exp} < 0.25$, the data lie within a scatter band of -25 to $+5\%$, irrespective of the channel geometry. The data of other channels omitted here also give better results than those of the annular channel, figure 9(b), in which the largest discrepancy (-25%) is observed. Thus, [14] together with [13] is seen to provide a good agreement with data of the mean void fraction for both bubble and slug flows in noncircular channels.

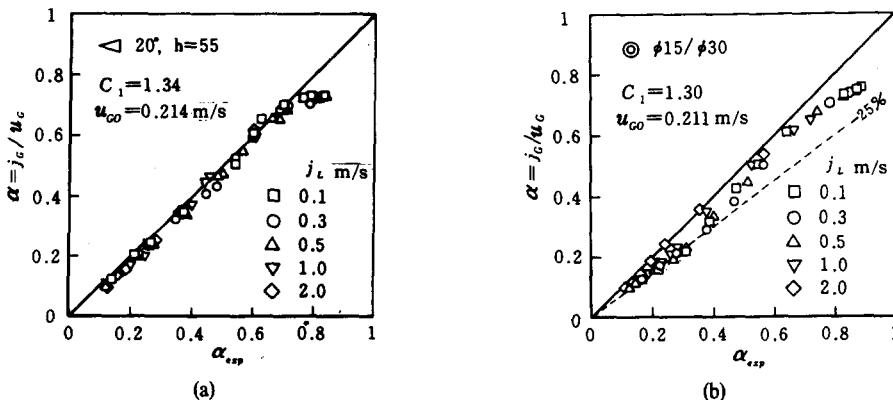


Figure 9. Comparison between experimental and predicted results for mean void fraction.

(b) *Cross-sectional distribution of void fraction.* A needle contact probe with a phase detecting electrode tip of 0.3 mm was used to determine the distribution of void fraction for typical flow patterns. A couple of results for the isosceles-triangular and the 17×50 mm rectangular channels are presented in figures 10(a)–(d), in an equi-void-contour map form. Figures 10(a) and (c) are the results for a bubble flow at $\alpha_{exp} \approx 0.15$. It is seen from these figures that in a bubble flow the local voids due to sliding bubbles (Sato *et al.* 1976) tend to peak near the walls

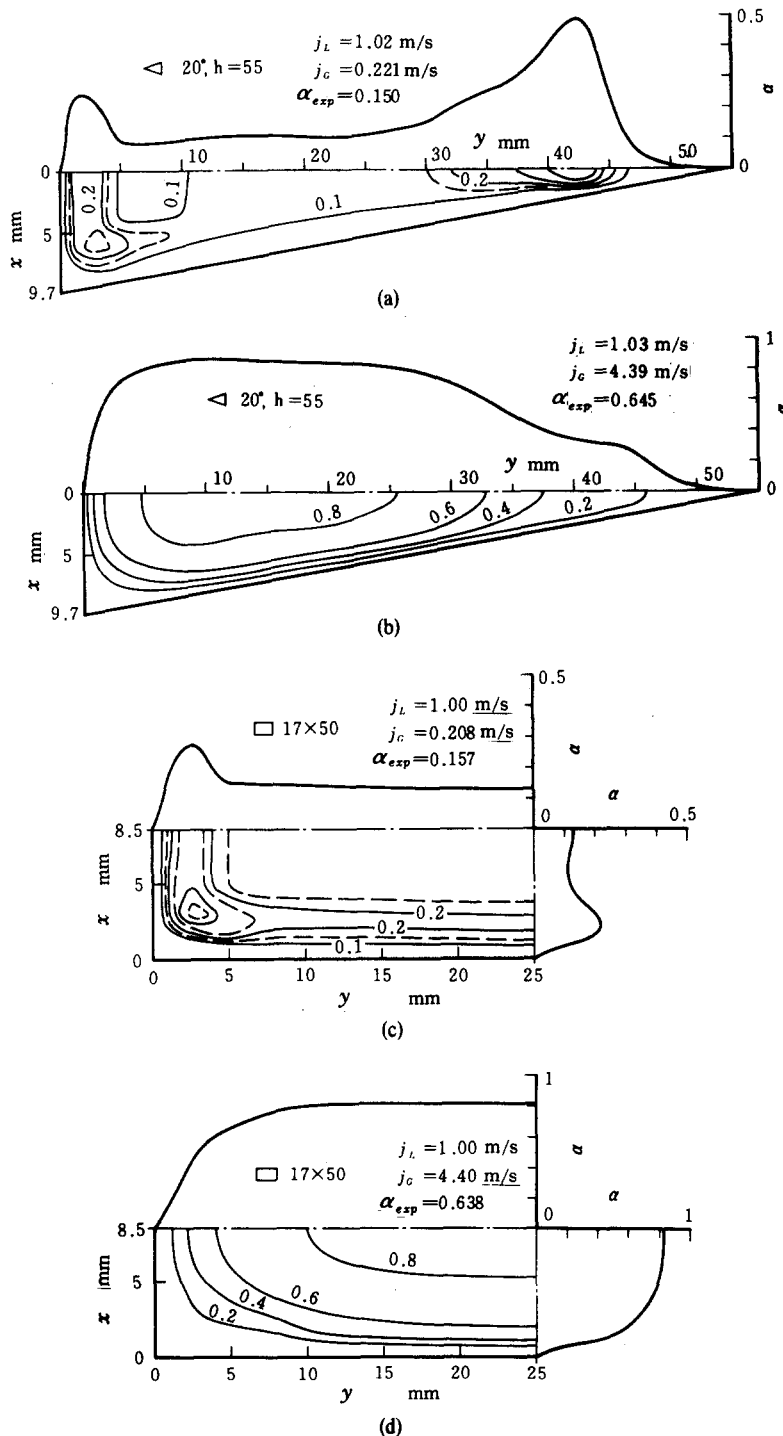


Figure 10. Equi-void-contour map for the isosceles-triangular and the 17×50 rectangular channels. ((a) and (c): bubble flow of $\alpha_{exp} \approx 0.15$, (b) and (d): slug flow of $\alpha_{exp} \approx 0.64$.)

and corners, and there is a basin in the central region. Both figures 10(b) and (d) pertain to a slug flow at $\alpha_{exp} \approx 0.64$. The peak value is observed at the same point at which the liquid velocity in turbulent flow has its maximum value in the cross section. These figures indicate that the gas phase flows in the central core while the liquid occupies the corners. This seems to be a variety of channeling phenomena, and thus unequal density and flow field along the periphery may result. Although such a phenomenon is outside the scope of this paper, it is felt that the understanding of it is one of the most important aspects of two-phase flow in noncircular channels.

Flow pattern transitions

As a final matter of interest, consideration may be given to the comparison of the flow pattern transition. Flow pattern was determined from the slugging frequency measured with a needle contact probe. The resulting flow pattern map for the seven channels is shown in figure 11 which employs the superficial velocities j_G and j_L as coordinates. Flows are classified into three primary patterns; bubble flow, slug flow and annular flow. The transition criteria of these flow patterns are described below.

If large gas bubble is defined as such a bubble that its longitudinal dimension exceeds the equi-periphery diameter D_e , then a corresponding slug interval which is the length from the nose of a large gas bubble to that of the succeeding one can be obtained from the frequency and the velocity u_G . It was found in this study that its average value decreases abruptly from infinity to about $10D_h$ in accordance with bubble to slug transition, and increases drastically from the order of $10D_h$ to infinity corresponding to transition from slug to annular flow. Based on these experimental findings, the criterion of bubble to slug transition is taken as the average slug interval to be $100D_h$ and that of slug to annular transition to be $1000D_h$.

From a comparison of the flow pattern boundaries in figure 11, there is little difference of the running among the test sections though the 7×20.6 mm rectangular one alone deviates somewhat from the others. Then, it appears that channel geometry itself has no considerable influence on flow pattern transition in noncircular channels, while channel dimension affects it in particular just above and below $D_h \approx 10$ mm.

CONCLUSIONS

The following conclusions may be drawn from the results of this study on single and two-phase flow in noncircular channels:

(1) The friction factor for fully developed turbulent single-phase flow has been correlated simply with Reynolds number by means of the turbulent geometry factor C_f ; $\lambda = C_f Re^{-0.25}$ analogous to the Blasius formula. C_f can be described empirically by [7] as a function of the laminar geometry factor C_l of the channel considered.

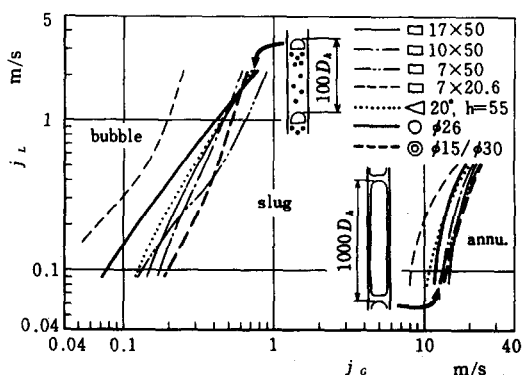


Figure 11. Flow pattern map.

(2) The two-phase frictional multiplier correlation proposed by Chisholm & Laird (1958) is also applicable to the frictional pressure drop in noncircular channels, if the relevant single-phase pressure drops for the both phases are determined.

(3) The rising velocity of gas bubbles in two-phase slug flows is given by [13], $u_G = C_1(j_G + j_L) + u_{GO}$. The coefficient C_1 is found to be nearly equal to the ratio of maximum to mean velocity in the cross section and u_{GO} , the velocity in a still water column, can be expressed approximately as $0.35\sqrt{gD_e}$.

(4) Data of the mean void fraction agree well with [14], $\alpha = j_G/u_G$, when the mean void fraction is less than 0.8 and the rising velocity of gas bubble is used for u_G .

(5) Channel geometry has no remarkable influence on the flow pattern transitions both from bubble to slug flow and from slug to annular flow when D_h is greater than about 10 mm.

REFERENCES

- ALY, A. M. M., TRUPP, A. C. & GERRARD, A. D. 1978 Measurements and prediction of fully developed turbulent flow in an equilateral triangular duct. *J. Fluid Mech.* **85**, 57–83.
- CARLSON, L. W. & IRVINE, JR., T. F. 1961 Fully developed pressure drop in triangular shaped ducts. *Trans. ASME, J. Heat Transfer* **83**, 441–444.
- CHISHOLM, D. & LAIRD, A. D. K. 1958 Two-phase flow in rough tubes. *Trans. ASME* **80**, 276–286.
- DAVIS, R. M. & TAYLOR, G. I. 1950 The mechanics of large bubbles rising through extended liquids and through liquids in tubes. *Proc. Roy. Soc.* **200**, Ser. A, 375–390.
- DUMITRESCU, D. T. 1943 Strömung an einer Luftblase in senkrechten Rohr. *ZAMM* **23**, 139–149.
- GRIFFITH, P. & WALLIS, G. B. 1961 Two-phase slug flow. *Trans. ASME, J. Heat Transfer* **83**, 307–320.
- GRIFFITH, P. 1964 The prediction of low-quality boiling voids. *Trans. ASME, J. Heat Transfer* **86**, 327–333.
- GUNN, D. J. & DARLING, C. W. W. 1963 Fluid flow and energy losses in non-circular conduits. *Trans. Inst. Chem. Engrs* **41**, 163–173.
- HARTNETT, J. P., KOH, J. C. Y. & MCCOMAS, S. T. 1962 A comparison of predicted and measured friction factors for turbulent flow through rectangular ducts. *Trans. ASME, J. Heat Transfer* **84**, 82–88.
- JONES, JR., O. C. 1976 An improvement in the calculation of turbulent friction in rectangular ducts. *Trans. ASME, J. Fluids Engineering* **98**, 173–181.
- JONSSON, V. K. & SPARROW, E. M. 1966 Experiments on turbulent-flow phenomena in eccentric annular ducts. *J. Fluid Mech.* **25**, 65–86.
- LAWN, C. J. & ELLIOTT, C. J. 1972 Fully developed turbulent flow through concentric annuli. *J. Mech. Engng Sci.* **14**, 195–204.
- LOCKHART, R. W. & MARTINELLI, R. C. 1949 Proposed correlation of data for isothermal two-phase, two-component flow in pipes. *Chem. Engng Prog.* **45**, 39–48.
- MALÁK, J., HEJNA, J. & SCHMID, J. 1975 Pressure losses and heat transfer in non-circular channels with hydraulically smooth walls. *Int. J. Heat Mass Transfer* **18**, 139–149.
- NICKLIN, D. J., WILKES, J. O. & DAVIDSON, J. F. 1962 Two-phase flow in vertical tubes. *Trans. Inst. Chem. Engrs* **40**, 61–68.
- NIKURADSE, J. 1930 Untersuchungen über turbulente Strömungen in nicht kreisförmigen Rohren. *Ingenieur-Archiv* **1**, 306–332.
- QUARMBY, A. 1967 An experimental study of turbulent flow through concentric annuli. *Int. J. Mech. Sci.* **9**, 205–221.
- REHME, K. 1971 Laminarströmung in stabbündeln. *Chemie-Ing.-Technik* **43**, 962–966.
- REHME, K. 1973 Simple method of predicting friction factors of turbulent flow in non-circular channels. *Int. J. Heat Mass Transfer* **16**, 933–950.

- SATO, Y., HONDA, T. & YOSHINAGA, T. 1976 An experimental investigation of air bubble motion in water streams in vertical ducts—I. On sliding bubble. (In Japanese), *Tech. Rep. Kumamoto University* **25**, 97–105.
- SHAH, R. K. & LONDON, A. L. 1978 *Laminar Flow Forced Convection in Ducts*. Academic Press, New York.
- TIEDT, W. 1968 Berechnung des laminaren und turbulenten Reibungswiderstandes konzentrischer und exzentrischer Ringspalte. *Chem.-Ztg./Chem.* **92**, 76–89.
- WHITE, E. T. & BEARDMORE, R. H. 1962 The velocity of rise of single cylindrical air bubbles through liquids contained in vertical tubes. *Chem. Engng Sci.* **17**, 351–361.